Indian Journal of Chemistry
Vol. 59B, July 2020, pp. 1043-1056

Synthesis, FT-IR, UV-VIS, DFT studies and SCXRD structure of 1-(tert-butyl) 3-ethyl-3-(hydroxy(thiophen-2-yl)methyl)piperidine-1,3-dicarboxylate

V D Singh[a], A Uppal[a], Kamni[a], Y Khajuria[a], R Srinivasan[b,c], B Narayana[b], B K Sarojini[d], Sumati Anthal[e] & Rajni Kant*[e]

[a] Department of Physics, Shri Mata Vaishno Devi University, Kakryal, Katra 182 320, India

[b] Department of Studies in Chemistry, Mangalore University, Mangalagangothri 574 199, India

[c] Aurigene Discovery Technologies Ltd., Electronics city, Phase-II, Bengaluru 560 100, India

[d] Department of Industrial Chemistry, Mangalore University, Mangalagangothri 574 199, India

[e] X-ray Crystallography Laboratory, Post-Graduate Department of Physics, University of Jammu, Jammu Tawi 180 006, India

E-mail: rkant.ju@gmail.com

Received 11 June 2019; accepted (revised) 8 July 2020

The crystal structure of 1-(tert-butyl) 3-ethyl 3-(hydroxy(thiophen-2-yl)methyl)piperidine-1,3-dicarboxylate ($C_{18}H_{25}NO_5S$) **I** has been determined by Single Crystal X-ray Diffraction (SCXRD) techniques. It crystallizes in the orthorhombic space group $Pca2_1$ with unit cell parameters a = 19.4502(13)Å, b= 6.3571(4)Å, c= 15.2577(10) Å and number of molecules per unit cell, Z = 4. The intensity data have been collected at room température (293 K) and the structure has been solved by direct methods. The full matrix least-squares refinement has converged the final R-value to 0.035 for 2251 observed reflections. The piperidine ring adopts a chair conformation. The structure is stabilized by two C–H…O (intermolecular interactions) and five C–H…O (intramolecular interactions). The structural and spectral studies of 1-(tert-butyl) 3-ethyl 3-(hydroxy(thiophen-2-yl)methyl)piperidine-1,3-dicarboxylate have been carried out by using both experimental and quantum chemical techniques.

Keywords: Crystal structure, direct methods, molecular packing, hydrogen bonding, spectral studies

The name piperidine is derived from the genus *Piper* which is the Latin word for pepper[1]. It occurs naturally in black pepper and has a burning peppery taste[2]. In pharmaceutical industry, it acts as a skeleton in some drugs like methylphenidate (as central nervous system stimulant), minoxidil (as an oral drug to treat high blood pressure), *etc*. and also as precursors in narcotic and physcotropic substances. β-Keto esters[3] are essential building blocks for the synthesis of a broad range of compounds with diverse activities and are conveniently used in the synthesis of α-halo and α-azido compounds[4] and also in various other formulations for related activities[5-9]. Taking into consideration the crystal structures of some related β-keto ester structures *viz*., *tert*-butyl 2-methyl-2-(4-methylbenzoyl)-propanoate[10], Zirconocene β-keto ester enolate[11] existing in the literature and the diverse pharmacological activities and potential such molecules hold[12-15], we report here the synthesis, X-ray crystal structure, spectral analysis and quantum chemical calculations of 1-(tert-butyl) 3-ethyl 3-(hydroxy(thiophen-2-yl)methyl)piperidine-1,3-dicarboxylate (**I**).

The quantum chemical calculations were performed to compute optimized geometry, atomic charges and thermodynamic properties using Hartree Fock Theory (HF) and Density Functional Theory (DFT) with 6-311G (d,p) basis set. The TD-DFT calculations were also carried out using 6-311G(d,p) basis set to determine the maximum absorption wavelength of the UV-Vis spectra for the title compound. The calculated HOMO-LUMO energies show that the charge transfer occurs within the molecule. The HOMO-LUMO study was extended to calculate ionization potential, electron affinity, global hardness, electron chemical potential and global electrophilicity. Stability of the molecule arises from hyper conjugative interactions; charge delocalization has also been analyzed using natural bond orbital (NBO) analysis. The temperature dependence of the thermodynamic properties of the optimized structure was obtained. The Fukui functions are also evaluated to describe the activity of the sites. There is a good agreement between calculated bond lengths and bond angles calculated by DFT theory and experimental data by XRD method.

Results and Discussion

SCXRD Structure of (I)

The molecular plot indicating atomic labels and as obtained using ORTEP-3[16] program is shown in Figure 1. The geometry of the molecule was calculated using PARST[17] and PLATON[18] software. The molecule consists of a five membered thiophen ring-A and six membered piperidine ring-B, bridged by carbonyl group. The structural parameters, including bond distances and angles show a normal geometry[19]. The double bonds C5 = O3, C11 = O2 and C16 = O5 are confirmed by their respective distances of 1.222(3) Å, 1.213(3) Å and 1.197(3) Å, respectively and are consistent with literature values[19]. Atoms O3 and O2 are twisted with respect to thiophene ring and piperidine ring, as indicated by the torsion angle values of C3–C4–C5-O3 [162.2(3)°] and O2-C11-N1-C9 [13.6(4)°] respectively as shown in Table I. Piperidine ring deviates significantly from planarity as indicated by the large values of torsion angles in it and adopts the *chair* conformation with mirror plane passing through atoms C8 and C10 [with asymmetry parameter $\Delta C_s(C8)$ = 4.211] and best two fold rotational axis bisecting the bonds C7-C8 and N1-C10 [with the asymmetry parameter $\Delta C_2(C7\text{-}C8)$ = 1.303].

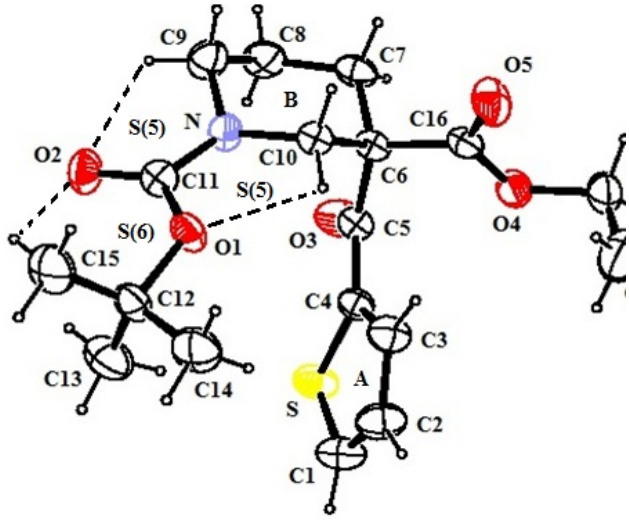

Figure 1 — ORTEP view of the molecule (I). Displacement ellipsoids are shown at 40% probability level. Hydrogen atoms are drawn at arbitrary radii. The graph-set motifs are also shown (dotted lines).

In the crystal structure, molecules are linked into a three-dimensional network by two intermolecular C–H…O and five intramolecular C–H…O hydrogen bonds. The two intermolecular hydrogen bonds link the molecules into infinite chains. Intra-molecular interactions C9–H9B…O2, C10–H10A…O1 and C15–H15C…O2 further provide stability to the molecules within themselves leading to the formation of S(5), S(5) and S(6) graph set motifs shown in Figure 1.

Details of intra/inter-molecular hydrogen bonding are given in Table II. No significant π-π stacking interactions were observed into the crystal structure. Molecular packing in the unit cell viewed down the *b*-axis is shown in Figure 2.

Optimized Geometry

The optimized structure of the title compound is shown in Figure 3. The optimized geometrical parameters (bond lengths and bond angles) calculated with HF and DFT methods using 6-311G(d,p) basis set are shown in Table III and Table IV, respectively. We have compared our results with the experimental data obtained by X-ray diffraction method. From the tables, it is clear that the experimental values are in

Table I — Selected torsion angles (°) (e.s.d.'s in parentheses)

S1–C4–C5–O3	-12.6(3)	C8–C9–N1–C11	-135.9(2)
S1–C4–C5–C6	166.58(2)	C10–N1–C11–O2	178.6(2)
C10–C6–C16–O5	-34.8(3)	O2–C11–O1–C12	12.0(4)
O3–C5–C6–C16	-112.8(3)	O4–C16–C6–C5	23.7(3)
C16–O4–C17–C18	81.1(3)	C3–C4–C5–O3	162.2(3)

Table II — Hydrogen bonding geometry (e.s.d.'s in parentheses)

D–H...A	D–H(Å)	H...A(Å)	D...A(Å)	D–H...A(°)
C3–H3...O3^{i}	0.93	2.45	3.221(3)	141
C8–H8B...O3	0.97	2.51	3.051(3)	115
C9–H9B...O2	0.97	2.40	2.800(4)	104
C10–H10A...O1	0.97	2.21	2.644(3)	106
C13–H13A...O2	0.96	2.53	3.062(4)	115
C15–H15C...O2	0.96	2.45	3.018(4)	118
C17–H17B...O2	0.97	2.49	3.389(4)	155

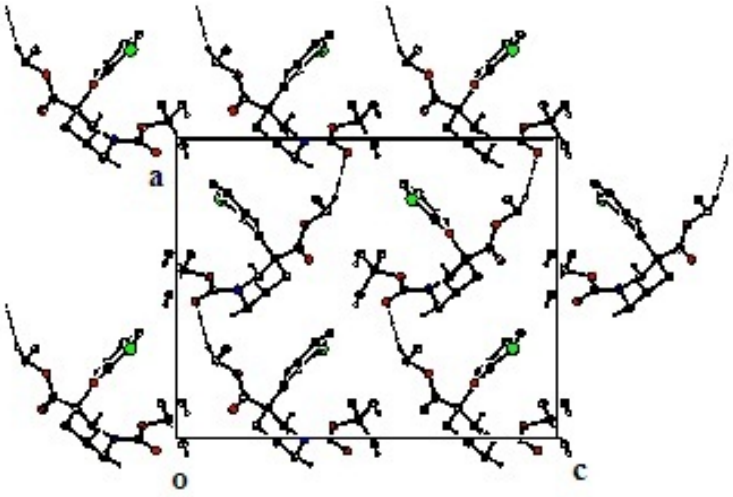

Figure 2 — Molecular packing along *b-axis*

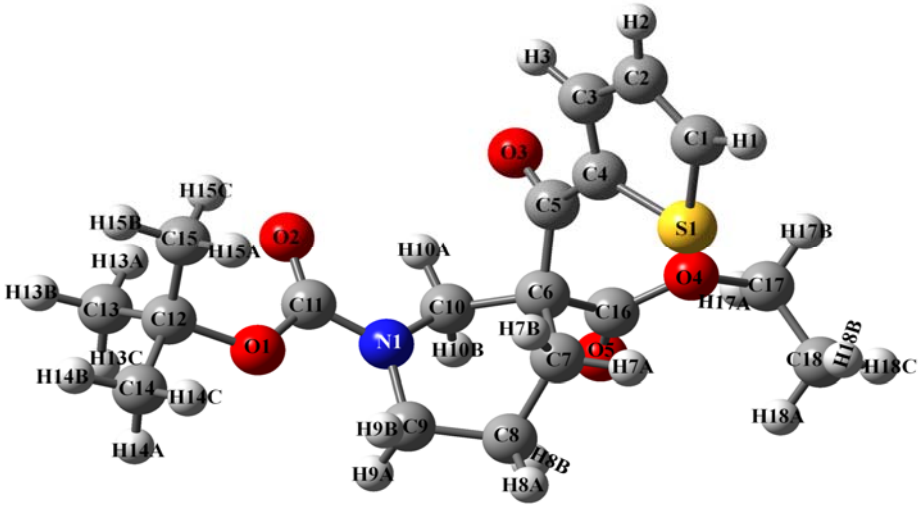

Figure 3 — Optimized structure of (I)

good comparison with the theoretical values obtained by both HF and DFT methods. The minimum energies of the optimized structure of the title molecule calculated by the HF/6-311G(d,p) and B3LYP/6-311G(d,p) are −1522.78113266a.u. and −1530.383 40751a.u. respectively. The difference in energy is about −7.60 a.u.

Atomic Net Charges

The calculations of effective atomic charges play a dominant role in the application of quantum mechanical calculations to molecular systems. The total atomic charges of 1-(tert-butyl) 3-ethyl 3-(hydroxy(thiophen-2-yl)methyl)piperidine-1,3-dicarboxylate obtained by Mulliken and NBO methods using HF/6-311G(d,p) and B3LYP/6-311G(d,p) level of theory are shown in Figure 4. The total atomic charge values are acquired by Mulliken population analysis by optimized geometry and natural charges are obtained by natural bond orbital analysis[20]. The Mulliken analysis is the most common population analysis method and these mulliken charges are calculated by determining the electron population of each atom as defined by the basis function. The hydrogen atom charges range in case of HF/6-311G(d,p) is from 0.099 to 0.176 where as the in case of B3LYP /6-311G(d,p) is from 0.088 to 0.148. All the hydrogen atoms and sulphur atom have a positive charge, which are acceptor atoms. The charge distribution for the oxygen atoms (O2, O1, O5, O4, O3) and nitrogen atom (N1) exhibit negative charge values which are donor atoms.

Table III — Calculated bond lengths (Å) of the molecule using HF/6-311G (d, p) and B3LYP/6-311G(d, p) basis set.

Atom no.	XRD	HF/6-311G(d,p)	B3LYP/6-311G(d,p)	Atom no.	XRD	HF /6-311G(d,p)	B3LYP/6-311G(d,p)
C8-C9		1.529	1.5351	C12-C14		1.5252	1.5294
C6-C10		1.5491	1.5581	O4-C17	1.463	1.4298	1.4543
C6-C5	1.550	1.5538	1.5643	C17-C18		1.5159	1.5188
C10-N1	1.460	1.4524	1.4579	C5-O3	1.222	1.1859	1.2139
N1-C9	1.461	1.4605	1.4681	C5-C4		1.4994	1.4878
N1-C11	1.355	1.3588	1.3714	C4-S1	1.727	1.7352	1.7495
C16-O5	1.197	1.1827	1.2055	S1-C1	1.695	1.7189	1.7241
C16-O4	1.331	1.319	1.3459	C1-C2		1.3458	1.3691
C11-O2	1.213	1.192	1.2147	C1-H1		1.0714	1.0798
C11-O1	1.344	1.3244	1.3583	C2-C3		1.4288	1.415
O1-C12	1.471	1.4477	1.4737	C2-H2		1.073	1.0817
C12-C13		1.5271	1.5313	C3-H3		1.0725	1.081

Table IV — Calculated bond angles (°) of the molecule using HF and DFT theory employing 6-311G (d, p) basis set.

Structural parameters	XRD	HF/6-311G(d,p)	B3LYP/6-311G(d,p)	Structural parameters	XRD	HF/6-311G(d,p)	B3LYP/6-311G(d,p)
C7-C8-C9		109.967	110.0918	C11-O1-C12	122.2	123.018	120.904
C9-C8-H8A		108.833	109.0001	O1-C12-C13		110.418	110.133
C8-C7-C6		110.735	110.6832	O1-C12-C15		110.428	110.195
C8-C7-H7B		108.818	109.1352	O1-C12-C14	102.0	102.662	102.447
C7-C6-C5		113.851	114.4134	C13-C12-C15		112.121	112.256
C10-C6-C16	107.24	108.984	108.3859	H13B-C13-H13A		108.812	108.929
C16-C6-C5	110.5	107.839	108.3064	C12-C15-H15C		111.450	111.056
C6-C10-N1		110.741	111.5451	H14B-C14-H14A		108.560	108.5476
N1-C10-H10A		108.809	108.236	C16-O4-C17	116.4	119.369	117.469
C10-N1-C9		116.898	117.158	O4-C17-C18		111.590	111.554
C10-N1-C11		119.120	119.085	O4-C17-H17A		108.757	108.337
C9-N1-C11	120.3	121.850	122.620	C18-C17-H17B		111.249	111.734
C8-C9-N1	110.2	109.241	109.340	H17A-C17-H17B		109.260	109.601
C8-C9-H9A		110.658	110.801	C6-C5-O3	120.1	118.953	118.547
C6-C16-O5	112.0	124.903	125.1507	C6-C5-C4		123.159	123.630
C6-C16-O4		111.191	111.043	O3-C5-C4	119.1	117.831	117.792
O5-C16-O4	124.2	123.858	123.769	C5-C4-S1	117.14	127.765	128.087
N1-C11-O2	124.2	124.488	124.677	C5-C4-C3		121.471	121.856
N1-C11-O1		110.926	110.222	S1-C4-C3	110.2	110.735	110.011
O2-C11-O1	125.3	124.585	125.100	C4-S1-C1	91.95	91.428	91.7322

FT-IR Spectroscopy and Vibrational Analysis

The compound 1-(tert-butyl) 3-ethyl 3-(hydroxy(thiophen-2-yl)methyl)piperidine-1,3-dicarboxylate($C_{18}H_{25}SNO_5$) consists of 50 atoms which undergoes (3N-6) 144 normal vibrational modes. The high accuracy prediction of vibrational calculations for a large number of compounds is done by DFT method[21]. The experimental FT-IR spectrum is presented in Figure 5 along with calculated FT-IR spectra using DFT method which indicates that the experimental frequencies correlate well with the calculated ones. Only those calculated frequencies are given in the Table V for which the corresponding experimental frequencies are observed. The calculated wavenumbers are usually higher than the corresponding experimental ones, due to the combination of electron correlation effects and insufficient basis set deficiencies. These discrepancies are removed either by computing anharmonic corrections explicitly or by introducing scalar field or even by direct scaling of the calculated wavenumbers with a proper scaling factor[22,23]. After applying the different scaling factors, the frequencies obtained by theoretical method are good in agreement with the

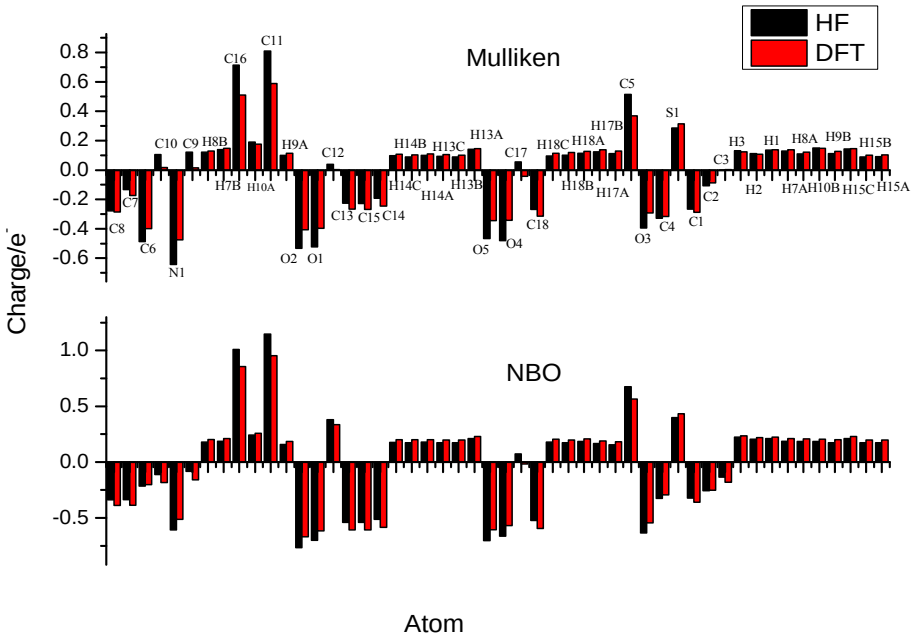

Figure 4 — Mulliken's plot and NBO plot of (I) with HF and DFT theory using B3LYP/6-311G(d,p) basis set

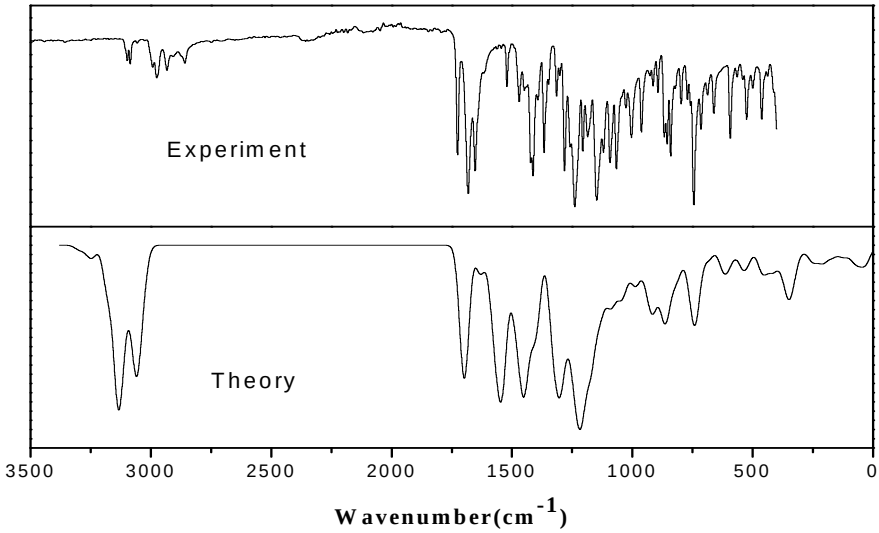

Figure 5 — Experimental and calculated FT-IR spectra of (I)

observed frequencies. In these calculations, the vibrational frequencies have been scaled by 0.967 in case of DFT/6-311G(d,p). The calculated frequency values are in good agreement with the experimental ones as shown in the Table V.

Natural Bond Orbital Analysis

The natural bond orbital calculation was performed using NBO program implemented in the Gaussian 09 package at the DFT/B3LYP level so as to understand intra-molecular delocalization or hyperconjugation. Natural bond orbital analysis is an efficient method that it gives information about interactions in both filled and virtual orbital spaces that could enhance the analysis of intra- and intermolecular interactions. The second-order Fock matrix was carried out to calculate the donor–acceptor interactions in the NBO analysis[24]. The corresponding results have been

Table V — Experimental and calculated (scaled) wavenumbers (in cm^{-1}) of (I)

Experimental frequencies	Unscaled frequencies DFT/6-311G(d,p)	Scaled frequencies DFT/6-311G(d,p)	IR intensities (KM/Mole)
3095	3298	3172	4.07
3083	3188	3066	10.12
2992	3104	2986	15.9
2972	3087	2969	12.85
2935	3053	2936	15.08
2855	3031	2915	30.32
1658	1705	1640	62.32
1646	1692	1627	81.4
1521	1583	1522	28.59
1472	1530	1471	13.17
1413	1468	1412	33.34
1365	1422	1367	7.64
1277	1331	1280	53.53
1238	1281	1232	43.2
1208	1259	1211	44.07
1159	1200	1154	59.44
1126	1171	1126	100
1091	1136	1092	28.03
1071	1112	1069	10.12
1023	1077	1036	24
1003	1052	1012	20.63
954	988	950	21.8
905	938	902	21.4
876	913	878	30.37
837	876	842	32.33
798	818	786	16.66
759	776	746	5.5
739	766	736	10.09
710	743	714	38.77
690	716	688	5.89
661	702	675	2.25
563	577	555	6.52
524	544	523	11.06
495	513	493	8.87
456	467	449	13
436	457	439	7.68

tabulated in Table VI. This table lists the major second order perturbation interactions along with the corresponding donor and acceptor NBOs. For each donor NBO (i) and acceptor NBO (j), the stabilization energy E(2) associated with delocalization ("2e-stabilization") is estimated. The electron delocalization from filled NBOs (donors) to the empty NBOs (acceptors) describes a conjugative electron transfer process between them. In NBO analysis larger the E(2) value, the more intensive is the interaction between electron donors and electron acceptors *i.e.* the more donating tendency from electron donors to electron acceptors and the extent of electron delocalization is greater. For each donor NBO (i) and acceptor NBO (j), the stabilization energy E(2) associated with i→ j delocalization, given by Equation

$$E(2) = \Delta E_{ij} = qi \frac{F(i,j)^2}{E_j - E_i}$$

Table VI — Second-order perturbation theory analysis of Fock Matrix in NBO basis corresponding to the intermolecular bonds of (I).

Donor (i)	ED(i)(e)	Acceptor (j)	ED(j)(e)	E(2) (KJ/mol)[a]	E(j) - E(i) (a.u)[b]	F(i,j) (a.u)[c]
σ (C8-C7)	1.97977	σ* (C7-C6)	0.02647	1.04	0.95	0.028
σ (C8-C7)	1.97977	σ* (C6-C5)	0.08003	2.44	0.96	0.044
σ (C8-C7)	1.97977	σ* (C9-H9A)	0.02441	1.44	1.02	0.034
σ (C8-C9)	1.98026	σ* (C7-H7A)	0.01268	1.83	1.03	0.039
σ (C8-C9)	1.98026	σ* (N1-C11)	0.07816	3.58	1.08	0.056
σ (C8-H8B)	1.97996	σ* (C7-H7B)	0.01632	2.86	0.91	0.046
σ (C8-H8A)	1.97542	σ* (C7-C6)	0.02647	3.55	0.84	0.049
σ (C8-H8A)	1.97542	σ* (N1-C9)	0.02803	3.19	0.85	0.046
σ (C7-C6)	1.95500	σ* (C8-H8A)	0.01085	1.37	1.02	0.034
π (C7-C6)	1.95500	π* (C16-O5)	0.21667	3.82	0.61	0.045
π (C7-C6)	1.95500	π* (C5-O3)	0.01044	1.82	1.20	0.042
σ (C7-H7B)	1.97664	σ* (C6-C16)	0.07541	2.71	0.85	0.043
σ (C7-H7A)	1.97805	σ* (C8-C9)	0.01458	2.83	0.88	0.045
σ (C6-C10)	1.96155	σ* (C7-H7A)	0.01268	1.50	1.01	0.035
σ (C6-C10)	1.96155	σ* (N1-C11)	0.07816	1.90	1.07	0.041
σ (C6-C10)	1.96155	σ* (C16-O4)	0.09911	2.58	0.96	0.045
σ (C6-C16)	1.95307	σ* (O4-C17)	0.03693	4.41	0.88	0.056
π (C6-C16)	1.95307	π* (C5-O3)	0.14650	2.80	0.65	0.039
π (C6-C5)	1.96793	π* (C16-O5)	0.02125	2.60	1.22	0.050
σ (C10-N1)	1.98177	σ* (C11-O1)	0.09807	2.68	1.10	0.049
σ (C10-H10A)	1.97762	σ* (N1-C9)	0.02803	4.74	0.84	0.056
σ (C10-H10B)	1.97921	σ* (C6-C5)	0.08003	2.55	0.84	0.042
π (N1-C9)	1.98452	π* (C11-O2)	0.06070	3.02	1.28	0.056
σ (C9-H9B)	1.98063	σ* (C10-N1)	0.02190	3.53	0.86	0.049
σ (C11-O1)	1.98924	σ* (C10-N1)	0.02190	2.96	1.25	0.055
σ (C13-H13C)	1.98602	σ* (C12-C15)	0.02972	3.90	0.87	0.052
σ (C14-H14B)	1.98238	σ* (O1-C12)	0.06791	4.43	0.75	0.052
σ (O4-C17)	1.98793	σ* (C6-C16)	0.07541	2.92	1.17	0.053
π (C4-C3)	1.79735	π* (C5-O3)	0.14650	18.50	0.30	0.067
π (C4-C3)	1.79735	π * (C1-C2)	0.31011	15.71	0.28	0.061
π (S1-C1)	1.98031	π * (C5-C4)	0.06451	4.21	1.12	0.062
π (C1-C2)	1.83757	π* (C4-C3)	0.33110	17.38	0.30	0.068
σ (C2-H2)	1.97475	σ* (S1-C1)	0.02126	4.60	0.76	0.053
σ (C3-H3)	1.97222	σ* (C4-S1)	0.03708	5.68	0.73	0.058
n(1)N1	1.71862	π* (C11-O2)	0.32763	44.97	0.34	0.111
n(2)O2	1.83611	π* (N1-C11)	0.07816	22.24	0.71	0.115
n(2)O1	1.83059	π * (C11-O2)	0.32763	30.83	0.40	0.104
n(2)O4	1.78852	π * (C16-O5)	0.21667	47.50	0.34	0.114
π* (C16-O5)	0.21667	π* (C5-O3)	0.14650	2.83	0.01	0.013
π* (C11-O2)	0.32763	π* (C11-O2)	0.06070	19.55	0.46	0.193
π* (C1-C2)	0.31011	π* (C4-C3)	0.31011	223.56	0.01	0.078

[a] E(2) means energy of hyperconjugative interactions

[b] Energy difference between donor and acceptor i and j NBO orbitals

[c] F(i,j) is the Fock matrix element between i and j NBO orbitals.

where q_i is the donor orbital occupancy, Ei, Ej are diagonal elements (orbital energies) and F(i, j) is the off-diagonal NBO Fock matrix element. In this compound, the interaction between the C1-C2 (NBO 604) and the C4-C3 antibonding (NBO 601) having the strongest stabilization, 223.56 KJ/mol. The intramolecular hyperconjugative interaction of π(C4-C3)→π*(C5-O3) and π(C1-C2)→π*(C4-C3) leading to a stabilization of 18.50 and 17.38 KJ/mol, respectively. Hence the charge transfer interactions explained above are responsible for the pharmaceutical and biological properties of $C_{18}H_{25}NO_5S$.

UV-Vis Spectral Analysis

Most of the absorption spectroscopy of the organic molecules is based on transitions π- π* and σ- σ* in the UV-Vis region[25,26]. The UV-Vis absorption spectrum of 1-(tert-butyl) 3-ethyl 3-(hydroxy(thiophen-2-yl)methyl)piperidine-1,3-dicarboxylate molecule has been recorded in the spectral range 190-800 nm. The most intense UV bands observed are due to excitation from Highest Occupied Molecular Orbital and Lowest Unoccupied Molecular Orbital (HOMO to LUMO). The electronic absorption spectra of title compound were calculated using the time-dependent density functional theory (TD-DFT) method based on 6-311G(d,p) level. The most intense UV bands at 216, 267, 308 and 345 nm are observed due to excitation from HOMO to LUMO as shown in Figure 6.

There is a good agreement between experimental and theoretical values obtained by TD-DFT method. The calculated absorption wavelengths, excitation energies, experimental wavelengths, oscillator strengths and their major contributions[27] are listed in Table VII. The calculated absorption spectrum shows that the maximum absorption wavelength corresponds to the electronic transition from HOMO-2→LUMO+1 with 98% contribution.

Thermodynamic Properties

Thermodynamic data coupled with density functional theory are very important to understand the chemical processes and properties of molecules. Using HF and DFT method, the thermodynamic parameters such as thermal energy, heat capacity,

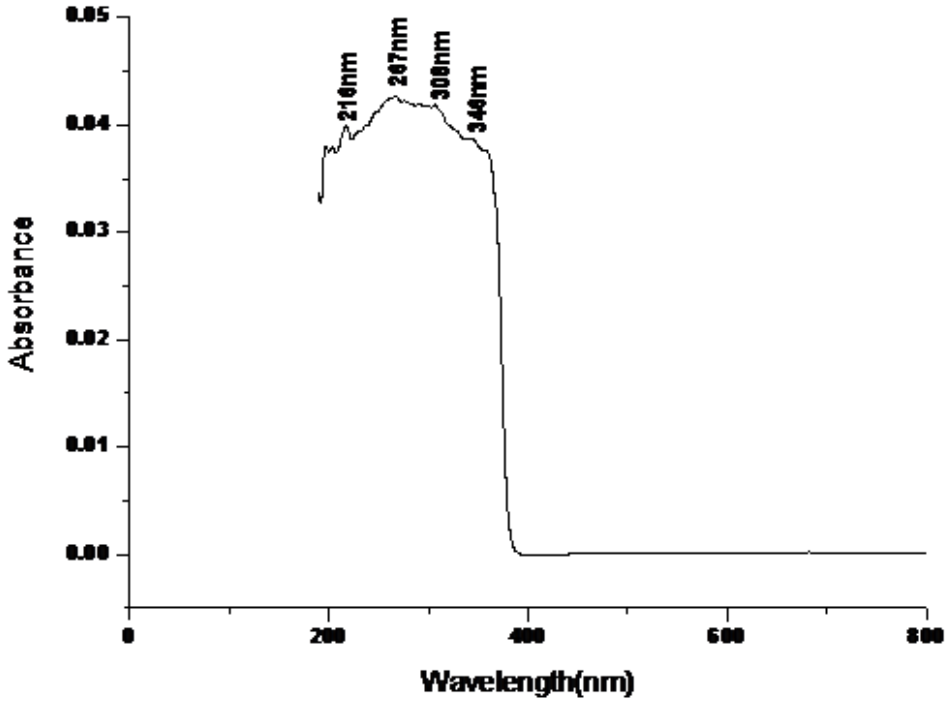

Figure 6 — UV-Vis spectra of (I)

Table VII — Theoretical and experimental electronic absorption spectra values of (I) using TD-DFT/6-311G(d,p) method and their assignments.

Wavelength λ(nm)		Energy(eV)	Oscillator strength(f)	Assignments [38]
Experiment	Theory	Theory	Theory	
216	225	5.49	0.0026	HOMO-5→LUMO(+41%)
267	266	4.65	0.0047	HOMO-2→LUMO+1(+98%)
308	317	3.91	0.004	HOMO→LUMO(+65%)+ HOMO-3→LUMO(+19%)
346	327	3.79	0.0052	HOMO-3→LUMO (+39%) + HOMO→LUMO (+41%)

entropy, rotational constants, dipole moment, *etc*. were calculated at 298.15K in ground state and are presented in Table VIII.

On the basis of vibrational analysis and statistical thermodynamics, the standard thermodynamic parameters like heat capacity, entropy and enthalpy for the title compound at B3LYP/6-311G(d,p) level were calculated within the temperature range from 100 to 700 K and are shown in Table IX.

Figure 7 shows a graphical correlation of thermodynamic parameters with temperature and it is observed that the value of these thermodynamic parameters augments with temperature because the molecular vibrational intensities increase with temperature[28].

The quadratic formulas were used to fit the correlation equations between different parameters such as heat capacity, entropy, enthalpy changes and temperatures and R is the corresponding fitting factor for these thermodynamic properties and the corresponding fitting equations are as follows:

$$C^{o}_{p,m} - 8.20431 + 0.33899T - 1.21253\times10^{-4}T^{2}(R^{2} = 0.99904)$$

$$S^{0}_{m} = 69.64503 + 0.40489T - 1.03296\times10^{-4}T^{2}(R^{2} = 0.99986)$$

$$H^{0}_{m} = 256.99802 + 0.02853T + 1.15836\times10^{-4}T^{2}(R^{2} = 0.99838)$$

HOMO-LUMO Analysis

Quantum chemical methods are important for collecting information about molecular structure and electrochemical behavior. A frontier molecular orbitals (FMO) analysis[29] was done for the title compound using B3LYP/6-311G(d,p) basis set. The highest occupied molecular orbital (HOMO) and lowest unoccupied molecular orbital (LUMO) are named as the frontier orbitals. The HOMO and LUMO are known as the electron donor and electron acceptor. The pictorial representation and the energy difference for title molecule are shown in Figure 8.

Table IX — Calculated thermodynamic properties at different temperatures at the DFT/6 311G(d,p) level of (I)

T(K)	$C°_{p.m}$(cal $mol^{-1}K^{-1}$)	$S°_{m}$(cal $mol^{-1}K^{-1}$)	$H°_{m}$(kcal mol^{-1})
100	42.249	108.335	261.094
200	70.214	147.780	266.745
298.15	96.900	180.659	277.720
300	98.055	182.281	275.149
400	125.278	214.848	286.336
500	149.029	245.875	300.086
600	168.707	275.206	316.005
700	184.908	302.775	333.712

Table VIII — Calculated thermodynamic parameters with HF and DFT theory using B3LYP function and 6-311G(d,p) basis set.

Thermodynamic Parameters (298K)	HF/6-311G(d,p)	B3LYP/6-311G(d,p)
SCF energy	-1522.78113266	-1530.38340751
Total energy (Thermal), E_{total}(Kcal mol^{-1})	292.654	274.969
Vibrational energy, E_{vib}(Kcal mol^{-1})	290.877	273.191
Zero point vibrational energy, E_0(Kcal mol^{-1})	277.20333	258.56713
Heat Capacity, C_v(Cal/Mol-Kelvin)	90.807	97.535
Entropy, S (Cal/Mol-Kelvin)	174.567	181.664
Rotational Constants (GHZ)		
A	0.32666	0.31953
B	0.12511	0.12311
C	0.10500	0.10358
Dipole moment (Debye)		
μ_x	1.7303	2.5906
μ_y	1.5736	1.1443
μ_z	4.6412	4.3932
μ_{total}	5.1972	5.2269

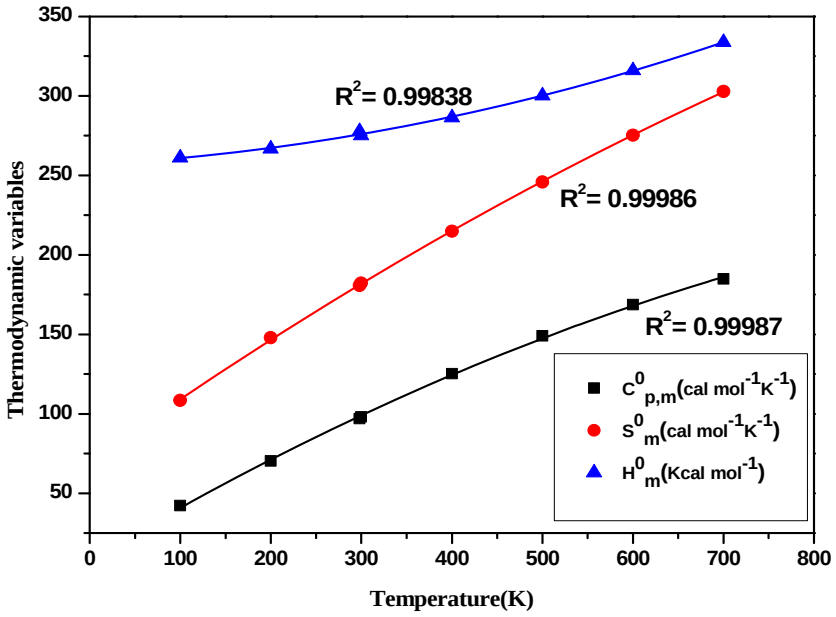

Figure 7 — Correlation graph between thermodynamic variables and temperature

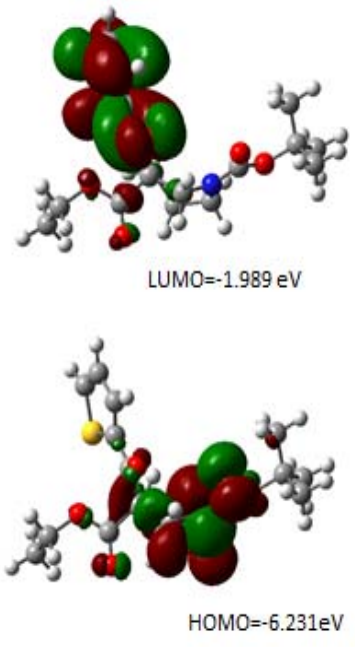

Figure 8 — HOMO-LUMO diagram for (I)

The HOMO is at −6.705 eV and is delocalized over the piperidine ring whereas the LUMO to be found at – 2.168eV which shows that the charge transfer to thiophene ring occurs within the molecule, and the energy gap is −4.53 eV. The frontier molecular orbital energy gap helps to characterize the chemical reactivity and kinetic stability of molecule[30,31]. The energy gap is an analytical parameter in determining molecular electrical transport properties and explains the eventual charge transfer interaction within the molecule. The HOMO and LUMO energies, the energy gap (ΔE), the ionization potential (I), the electron affinity (A), global hardness(η) chemical potential (μ), global electrophilicity(ω) for molecule have been calculated at the same level and the results are given in Table X.

Fukui Function

Density Functional Theory is a powerful tool for the study of reactivity and selectivity in a molecule[32]. The most basic and commonly used local reactivity parameter is the Fukui function. Change in the density function with change of number of electrons in the molecule when the positions of nuclei remains unchanged has been termed as Fukui function[33,34]. Fukui function gives us information about electrophilic/nucleophilic power of a given atomic site in a molecule. The condensed Fukui functions on the j^{th} atom site can be expressed as:

$$f_j^+ = q_j(N+1) - q_j(N)$$

$$f_j^0 = \frac{1}{2}[q_j(N+1) - q_j(N-1)]$$

$$f_j^- = q_j(N) - q_j(N-1)$$

Where, f_j^+ for nucleophilic attack, f_j^- for electrophilic attack and $f_j°$ for free radical. In these equations, q_j is the atomic charge at the j^{th} atomic site in the neutral (N), anionic (N+1) or cationic (N-1) chemical species. The atomic charges either calculated by natural population analysis (NPA) or by Mulliken population analysis (MPA) have been used to calculate the Fukui function. In the present study the values of Fukui Function calculated from the NBO charges. Dual descriptor $\Delta f(r)$[35] for the calculation of nucleophilicity and electrophilicity is defined as the difference between the nucleophilic and electrophilic Fukui function and is given by the equation:

$$\Delta f(r) = f_j^+ - f_j^-$$

If $\Delta f(r) > 0$, then the site is prone for nucleophilic attack, if $\Delta f(r) < 0$, then the site is for electrophilic attack. The condensed Fukui functions (f^+_j), (f^-_j) and dual descriptor $\Delta f(r)$ are given in Table XI. For this molecule, N1, O2, O1, C15, O5, O3, S1, C2 and hydrogen atoms are prone for nucleophilic attack as $\Delta f(r) > 0$ whereas C8, C10, C16, C12, O4, C18, C5, C3 are prone for electrophilic attack.

Table X — HOMO-LUMO and other related molecular properties

Molecular parameters (eV)	B3LYP/6-311G(d,p)
E_{LUMO}	-1.989
E_{HOMO}	-6.231
E_{LUMO}- E_{HOMO}	4.242
Ionization potential (I)	6.231
Electron affinity (A)	1.989
Global hardness (η)	2.121
Chemical potential (μ)	4.11
Softness(S)	0.235
Global Electrophilicity (ω)	3.98

Experimental Section

Synthesis

To a solution of 1-(*tert*-butyl) 3-ethyl 3-(hydroxy(thiophen-2-yl)methyl)piperidine-1,3-dicarboxylate (9.0 g, 24.35 mmol, 1 eq) in DCM (150 mL), MnO_2(72 g, 828 mmol, 32.5 eq) was added and stirring continued at RT for 3-4 h. After examination of the completion of reaction by TLC, the reaction mixture was filtered through a Celite bed and the filtrate was concentrated to give the title product (8.1 g, 90.5% yield). Single crystals appropriate for X-ray diffraction study were developed by slow evaporation technique from DCM

Table XI — Fukui indices for nucleophilic and electrophilic attacks on atoms calculated from natural population analysis at DFT/6-311G(d,p)

Atom	f^+	f^-	$f°$	$\Delta f(r)$
C8	0.19388	-0.19431	0.38819	-0.00021
C10	0.08155	-0.09187	0.17342	-0.00516
N1	0.58904	-0.26287	0.85191	0.163085
H8B	-0.09314	0.10544	-0.19858	0.00615
C16	-0.43385	0.41922	-0.85307	-0.00731
O2	0.46702	-0.332	0.79902	0.06751
O1	0.32708	-0.30663	0.63341	0.010375
C12	-0.16928	0.16653	-0.33581	-0.00137
C15	0.30441	-0.30402	0.60843	0.000195
H13B	-0.08777	0.10445	-0.19222	0.00834
O5	0.32896	-0.28118	0.61014	0.02389
O4	0.28777	-0.29492	0.58269	-0.00358
C18	0.29648	-0.29938	0.59586	-0.00145
C5	-0.30372	0.24927	-0.55299	-0.02723
O3	0.3458	-0.31131	0.65711	0.017245
C4	0.23622	-0.16372	0.39994	0.03625
S1	-0.21098	0.24569	-0.45667	0.017355
C2	0.13556	-0.08507	0.22063	0.025245
C3	0.12428	-0.12491	0.24919	-0.00031
H10B	-0.05677	0.11207	-0.16884	0.02765

solvent. The synthetic path for the preparation of the compounds is given in Figure 9.

SCXRD Structure Analysis and Refinement

X-ray intensity data of the crystal of dimensions 0.30×0.20×0.10 mm^3 having clear morphology were collected on *X'calibur* CCD area-detector diffractometer equipped with graphite monochromated Mo*Kα* radiation (λ = 0.71073 Å)[36]. The intensities were measured by making use of ω scan mode for the diffraction angle ranging from 3.63 to 25.98°. X-ray intensity data for 4774 reflections were collected at 293(2) K and out of these reflections 2798 were found unique. 2251 reflections were treated as observed by using the criterion I >2σ (I). Data were corrected for Lorentz-polarization and absorption factors.

Direct methods were used to solve the structure by using SHELXS97[37] and was refined using SHELXL97[37]. All non-hydrogen atoms of the molecule were located in the best E-map. All the hydrogen atoms were geometrically fixed and allowed to ride on the corresponding carbon with C-H= 0.93-0.97Å and U_{iso}= 1.2 U_{eq}(*C*), except for the methyl groups where U_{iso}(H) = 1.5 U_{eq}(*C*). The final refinement cycles converged to an R-factor of 0.0354 [$wR(F^2)$ = 0.0611] for 2251 observed reflections. Residual electron densities ranges from -0.205 to 0.162 $eÅ^{-3}$. Geometrical calculations of the molecule were done using the WinGX[38], PARST[17] and PLATON[18] softwares. The crystallographic and refinement data of the crystal is given in Table XII.

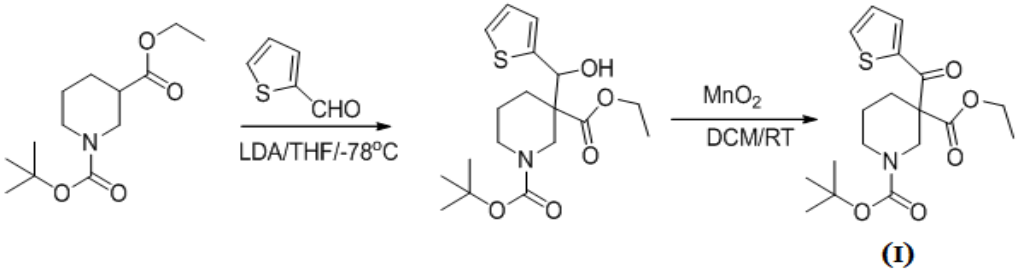

Figure 9 — Reaction scheme for the synthesis of (**I**)

Table XII — Precise crystallographic data and structure refinement parameters for $C_{18}H_{25}NO_5S$

CCDC Number	1543225
System, Space group, Z	Orthorhombic, $Pca2_1$, 4
a, *b*, *c* Å	19.4502(13), 6.3571(4), 15.2577(10)
β, deg	90.00(0)
V, $Å^3$	1886.6(2)
Radiation, λ, Å	0.71073
μ, mm^{-1}	0.199
T, K	293(2)
Sample size, mm^3	0.30×0.20×0.10
Diffractometer	*X'calibur* Sapphire3 CCD area-detector
Scan mode	ω scan
Absorption correction	multi-scan
T_{min}, T_{max}	0.87605, 1.00000
θ range, deg	3.63→25.98
h, k, l ranges	*h* = -23→23, *k* = -3 →7, *l* = -12→18
Reflections total/unique	4774/ 2798
Reflections observed [I > 2σ(I)]	2251
R_{int}	0.0331
R_{sigma}	0.0505
F(000)	784
R	0.0354
$wR(F^2)$	0.0655
$(\Delta/\sigma)_{max}$	0.00
Number of refined parameters	230
S	0.913
$\Delta\rho_{max}/\Delta\rho_{min}$, $e/Å^3$	0.162/-0.205
Programs used	SHELXS97, SHELXL97, PARST, PLATON, ORTEP.

Experimental and Computational Details

Shimadzu IR- Tracer having spectral resolution of 1cm^{-1} has been used to record the FT-IR spectrum of the compound in the spectral range of 4000-400 cm^{-1}. ISR assembly attached with Shimadzu UV-2600 Double beam spectrophotometer in the spectral region 190-1400 nm was used to record the Electronic absorption spectrum. All the calculations reported in this work have been done using HF and DFT[39] methods with Gaussian 09W[40]. The first optimization of the geometry takes place at Hartree-Fock level using 6-311G(d,p) basis set and then reoptimizes it by using DFT and DFT employed the three-parameter hybrid functional(B3)[41,42] for the exchange part and the Lee-Yang-Parr (LYP) correlation function[43], using standard 6-311G(d,p) basis set. For the calculations of vibrational frequencies, thermodynamic parameters, Fukui functions and other molecular properties, the optimized structural parameters have been evaluated. In this paper, the net charges were calculated using Mulliken population method and natural population analysis. The calculated natural atomic charges values were further used to calculate Fukui Functions. The electronic properties were calculated using time-dependent DFT (TD-DFT)[44-46] with 6-311G(d,p) basis set to investigate the properties of ground and excited state. The experimental data and TD-DFT results of the 1-(*tert*-butyl) 3-ethyl 3-(hydroxy (thiophen-2-yl)methyl) piperidine-1,3-dicarboxylate have been compared.

Conclusions

1-(*tert*-Butyl)-3-ethyl-3-(hydroxy(thiophen-2-yl)-methyl)piperidine-1,3-dicarboxylate has been synthesized and characterized by FT-IR, UV-Vis and single crystal XRD. The structural geometrical parameters, vibrational, NBO, HOMO-LUMO analysis, and the thermodynamic properties of the title molecule were calculated on the basis of HF and DFT at B3LYP/6-311G(d,p) basis sets. Experimental FT-IR spectra analyses are in good agreement with the calculated vibrational frequencies. NBO analyses exhibit hyper conjugative interaction and stabilization of the molecule. The correlations between the statistical thermodynamics and temperature are obtained and show that the increase in temperature causes the increase in heat capacities, entropies and enthalpies. The Fukui functions are evaluated to describe the possible sites of nucleophilic and electrophilic attacks in the molecule.

Acknowledgements

Rajni Kant acknowledges research support received under DST Research Project No: EMR/2014/000467. Kamni is thankful to the UGC for funding under Project No. MRP-MAJOR-PHYS-2013–26952 (RP-88).

References

1 Welcher F J, *Organic Analytical Reagents* (D Nostrand V), p.149 (1947).
2 Senning A, *Elsevier's Dictionary of Chemoetymology* (Elsevier, Amsterdam) (2006).
3 Fenaroli G, Bellanca N, Burdock G A & Furia T A, *Fenaroli's Handbook of Flavor Ingredients*, Second Edition, (CRC Press, Boca Raton, Fla, USA) (1975).
4 Benetti S, Romagnali R, Derisi C, Spalluto G & Zanirato V, *Chem Rev*, 95 (1995) 1065.
5 Galligan M J, Akula R & Ibrahim H, *Org Lett*, 16 (2014) 600.
6 Luo L C, Meng L L, Sun Q, Ge Z M & Li, *Tetrahedron Lett*, 55 (2014) 259.
7 Bonne D, Coquerel Y, Constantieux T & Rodriguez J, *Tetrahedron*: *Asymmetry*, 21 (2010) 1085.
8 Rao G B D, Acharya B N & Kaushik M P, *Tetrahedron Lett*, 54 (2013) 6644.
9 Russowsky D, Canto R F S, Sanches S A A, D'oca M G M, Fatima A D, Pilli R A, Konhn L K, Antonia M A & Carvalho J E D, *Bioorg Chem*, 34 (2006) 173.
10 Srinivasan R, Narayana B, Sarojini B K, Bhanuprakash V, Raj C G D & Nayak P S, *Lett Drug Des Disc*, 13 (2016) 149.
11 Srinivasan R, Narayana B, Samshuddin S & Sarojini B K, *Molbank*, M757 (2012a).
12 Srinivasan R, Narayana B, Samshuddin S & Sarojini B K, *Molbank*, M757 (2012b).
13 Srinivasan R, Narayana B, Samshuddin S & Sarojini B K, *Molbank*, M757 (2012c).
14 Srinivasan R, Narayana B, Samshuddin S & Sarojini B K, *Molbank*, M757 (2012d).
15 Gould G B, Jackman B G, Logue M W, Luck R L, Pignotti L R, Smith A R & White N M, *Acta Cryst*, E66 (2010) o491.
16 Farrugia L J, *J Appl Crystallogr*, 30 (1997) 565.
17 Nardelli M, *J Appl Crystallogr*, 28 (1995) 659.
18 Spek A L, *Acta Crystallogr*, D65 (2009) 148.
19 Allen F H, Kennard O, Watson D G, Brammer L, Orpen A G & Taylor R, *J Chem Soc Perkin Trans 2*, (1987) S1.
20 Mulliken R S, *J Chem Phys*, 23 (1955) 1833.
21 Karabacak M, Sinha L, Prasad O, Asiri A M, Cinar M & Shukla V K, *Spectrochim Acta*, A123 (2014) 352.
22 Keresztury G, Holly S, Varga J, Besenyei G, Wang A Y & Durig J R, *Spectrochim Acta*, A49 (1993) 2007.
23 Keresztury G, 'Raman Spectroscopy: Theory', in *P R Handbook of Vibrational Spectroscopy*, edited by Chalmers J M and Griffith (John Wiley and Sons, New York) (2002).
24 Szafran M, Komasa A & Bartoszak-Adamska E, *J Mol Struct*, 827 (2007) 101.
25 Silverstein R M, Bassler G C & Morrill T C, *Spectrometric Identification of Organic Compounds* (John Wiley, Chichester) (1991).

26 Cotton F A & Wilkinson C W, *Advanced Inorganic Chemistry*, 3rd edn. (Interscience Publishers, New York) (1972).
27 Gorelsky S I, SWizard program, http://www.sg-chem.net/.
28 Ott J B & Boerio-Goates J, *Chemical Thermodynamics*: *Principles and Applications* (Academic Press, San Diego) (2000).
29 Sheikhi M & Sheikh D, *Rev Roum Chim*, 59 (2014) 761.
30 Kavitha E, Sundaraganesan N & Sebastian S, *Indian J Pure Appl Phys*, 48 (2010) 20.
31 Jayaprakash A, Arjunan V & Mohan S, *Spectrochim Acta*, A81 (2011) 620.
32 Parr R G & Yang W, *Density Functional Theory of Atoms and Molecules* (Oxford University Press, New York) (1989)
33 Ayers P W & Parr R G, *J Am Chem Soc*, 122 (2000) 2010.
34 Parr R G & Yang W J, *J Am Chem Soc*, 106 (1984) 511.
35 Morell C, Grand A & Toro-Labbe A, *J Phys Chem*, A109 (2005) 205.
36 Stuhldreier T, Keul H & Hocker H, *Organometallics*, 19 (2000) 5231.
37 Sheldrick G M, *Acta Cryst*, A64 (2008) 112.
38 Farrugia L J, *J Appl Crystallogr*, 32 (1999) 837.
39 Hohenberg P & Kohn W, *Phys Rev* B, 136 (1964) 864.
40 Becke A D, *J Chem Phys*, 98 (1993) 5648.
41 Becke A D, *Phys Rev A*, 38 (1988) 3098.
42 Lee C, Yang W & Parr R G, *Phys Rev B*, 37 (1988) 785.
43 Frisch M J, Trucks G W, Schlegel H B, Scuseria G E, Robb M A, Cheeseman J R, Scalmani G, Barone V, Mennucci B, Petersson G A, Nakatsuji H, Caricato M, Li X, Hratchian H P, Izmaylov A F, Bloino J, Zheng G, Sonnenberg J L, Hada M, Ehara M, Toyota K, Fukuda R, Hasegawa J, Ishida M, Nakajima T, Honda Y, Kitao O, Nakai H, Vreven T, Montgomery Jr J A, Peralta J E, Ogliaro F, Bearpark M, Heyd J J, Brothers E, Kudin K N, Staroverov V N, Kobayashi R, Normand J, Raghavachari K, Rendell A, Burant J C, Iyengar S S, Tomasi J, Cossi M, Rega N, Millam N J, Klene M, Knox J E, Cross J B, Bakken V, Adamo C, Jaramillo J, Gomperts R, Stratmann R E, Yazyev O, Austin A J, Cammi R, Pomelli C, Ochterski J W, Martin R L, Morokuma K, Zakrzewski V G, Voth G A, Salvador P, Dannenberg J J, Dapprich S, Daniels A D, Farkas O, Foresman J B, Ortiz, Cioslowski J & Fox D J, Gaussian 09, Revision **A**.**1**, Gaussian, Inc., Wallingford, CT (2013).
44 Bader R F W, *Atoms in Molecules*: *A Quantum Theory* (Oxford University Press, Oxford, UK) (1990).
45 Bauernschmitt R & Ahlrichs R, *Chem Phys Lett*, 256 (1996) 454.
46 Kose E, Atac A, Karabacak M, Karaca C, Eskici M & Karanfil A, *Spectrochim Acta A*, 97 (2012) 435.